HHS Public Access

Author manuscript

Neuroimage. Author manuscript; available in PMC 2021 July 15.

Published in final edited form as:

Neuroimage. 2020 July 15; 215: 116792. doi:10.1016/j.neuroimage.2020.116792.

Intra- and interhemispheric white matter tract associations with auditory spatial processing: Distinct normative and aging effects

James W. Dias*, **Carolyn M. McClaskey**, **Mark A. Eckert**, **Jens H. Jensen**, **Kelly C. Harris**

Medical University of South Carolina, USA

Abstract

Declining auditory spatial processing is hypothesized to contribute to the difficulty older adults have detecting, locating, and selecting a talker from among others in noisy listening environments. Though auditory spatial processing has been associated with several cortical structures, little is known regarding the underlying white matter architecture or how age-related changes in white matter microstructure may affect it. The arcuate fasciculus is a target for understanding age-related differences in auditory spatial attention based on normative spatial attention findings in humans. Similarly, animal and human clinical studies suggest that the corpus callosum plays a role in the cross-hemispheric integration of auditory spatial information important for spatial localization and attention. The current investigation used diffusion imaging to examine the extent to which age-group differences in the identification of spatially cued speech were accounted for by individual differences in the white matter microstructure of the right arcuate fasciculus and the corpus callosum. Higher right arcuate and callosal fractional anisotropy (FA) predicted better segregation and identification of spatially cued speech across younger and older listeners. Further, individual differences in callosal microstructure mediated age-group differences in auditory spatial processing. Follow-up analyses suggested that callosal tracts connecting left and right pre-frontal and posterior parietal cortex are particularly important for auditory spatial processing. The results are consistent with previous work in animals and clinical human samples and provide a cortical mechanism to account for age-related deficits in auditory spatial processing. Further, the results suggest that both intrahemispheric and interhemispheric mechanisms are involved in auditory spatial processing.

Keywords

Corpus callosum; Superior longitudinal fasciculus; Arcuate fasciculus; Aging; Auditory spatial processing; Auditory spatial attention; Speech in noise

*Corresponding author. Medical University of South Carolina, Department of Otolaryngology, 135 Rutledge Avenue, MSC 550, Charleston, SC 29425-5500. diasj@musc.edu (J.W. Dias).

CRediT authorship contribution statement

James W. Dias: Conceptualization, Methodology, Formal analysis, Investigation, Data curation, Writing - original draft, Visualization. **Carolyn M. McClaskey:** Investigation, Data curation, Writing - review & editing. **Mark A. Eckert:** Conceptualization, Methodology, Writing - review & editing, Visualization. **Jens H. Jensen:** Methodology, Software, Resources, Writing - review & editing. **Kelly C. Harris:** Conceptualization, Methodology, Investigation, Resources, Data curation, Writing - review & editing, Supervision, Project administration, Funding acquisition.

Declaration of competing interest

None.

1. Introduction

Interaural differences in sound intensity and timing provide important spatial information for detecting, locating, selecting, and attending to a talker from among others in noisy listening environments (for a review, see Rauschecker, 2018). Such “cocktail party” scenarios can prove more challenging when auditory spatial processing degrades with age (for a review, see Freigang et al., 2015). Though several cortical structures important for audition, spatial perception, and attention are involved in auditory spatial processing, little is known regarding the underlying interhemispheric and intrahemispheric white matter architecture or how age-related changes in white matter structure may affect auditory spatial perception.

2. Age-related deficits in auditory spatial processing

Older listeners, even those with clinically normal audiometric thresholds, typically exhibit some level of difficulty identifying the location of an auditory signal (for a review, see Freigang et al., 2015) and attending to a target signal in the presence of spatially-incongruent competitors (Grady et al., 2007; Singh et al., 2008). These age-related deficits in auditory spatial localization and attention are thought to contribute to the well-established difficulties older listeners have communicating with others in complex listening environments (e.g., Föllgrabe et al., 2015; Dubno et al., 1984). Individual differences in auditory nerve and auditory brainstem function contribute to auditory spatial processing (e.g., Bharadwaj et al., 2015; Harris et al., 2017). However, cortical asymmetries and cross-hemispheric processing of spatial information have been found to be important for auditory spatial localization and attention (e.g., Barrick et al., 2006; Grady et al., 2011; Greenwald and Jerger, 2001; Lewald et al., 2016; Rauschecker, 2018). For example, the event-related potentials (ERPs) of older listeners performing an interaural auditory spatial selective attention task exhibited longer cross-hemispheric latencies and reduced amplitude asymmetries, which were hypothesized to stem from age-related degradation of the corpus callosum (Greenwald and Jerger, 2001).

3. Interhemispheric auditory spatial processing

The corpus callosum, the primary commissure allowing for the interhemispheric transfer of lateralized information, may serve a role in processing interaural information important for auditory spatial perception. Extracellular recordings in cats (Poirier et al., 1995) and mice (Rock and Apicella, 2015) suggest that the corpus callosum transfers information for sound localization across hemispheres. Human callosotomy patients and listeners with callosal agenesis exhibit significant deficits in their ability to localize and attend to sounds based on interaural timing differences (Hausmann et al., 2005; see also Lepore et al., 2002; Poirier et al., 1993). The extant animal and human studies, together with the considerable normative and age-related variation in callosal morphology (Nusbaum et al., 2001; Pfefferbaum et al., 2004), suggest that varied auditory spatial attention may be explained by individual differences in callosal morphology.

4. Intrahemispheric auditory spatial processing

Studies of stroke patients with *visual* spatial neglect have found that patients with lesions in the superior longitudinal fasciculus (SLF), an association fiber tract connecting frontal, parietal, temporal, and occipital cortices, exhibit moderate to severe hemifield neglect, which is typically observed as left-hemifield neglect associated with right SLF damage (e.g., Carter et al., 2017; Chechlacz et al., 2010; Chechlacz et al., 2013; Karnath and Rorden, 2012; Karnath et al., 2009; Meola et al., 2015; Molenberghs et al., 2012; Thiebaut de Schotten et al., 2012; Urbanski et al., 2011; Vaessen et al., 2016). These studies and the broader attention literature suggest that the SLF supports visual spatial attention. However, few studies have examined the generalizability of the SLF to the processing of spatial information accessible from other sensory modalities, nor have many studies examined the degree to which individual differences in intact SLF structure relate to spatial processing in healthy individuals (e.g., Suchan et al., 2014).

It has been hypothesized that the right arcuate fasciculus, the segment of the SLF connecting frontal, parietal, and temporal cortices, is important for transferring auditory spatial information to cortical areas typically found to be involved in spatial attention (Barrick et al., 2006; Griffiths et al., 2000; Griffiths et al., 1998; Huang et al., 2014). However, few studies have directly investigated the degree to which individual differences in right arcuate structure relate to auditory spatial processing.

5. Current investigation

Interhemispheric and intrahemispheric processing of auditory spatial information suggests that both interhemispheric and intrahemispheric white matter tracts play a role in auditory spatial processing. Past studies have suggested that the corpus callosum and the right arcuate fasciculus are involved, but the degree to which individual differences in intact callosal and arcuate structure relate to the auditory spatial processing of younger and older listeners has not been thoroughly investigated. Importantly, even healthy older adults typically exhibit evidence of degraded white matter microstructure, characterized by reduced fractional anisotropy (FA) and increased mean diffusivity (MD), which is thought to result from demyelination, reduced cellular membrane density, and changes to myelin structure and fluid viscosity (Alexander et al., 2011; Feldman et al., 2010; Ota et al., 2006; Salat et al., 2005; Teubner-Rhodes et al., 2016). Age-related differences in callosal and right arcuate microstructure and their apparent role in auditory spatial processing guides the hypothesis that age-related differences in auditory spatial processing can be accounted for, at least partially, by individual differences in callosal and right arcuate microstructure. To test this hypothesis, we first used diffusion-weighted magnetic resonance imaging (DW-MRI) to compute scalars for the callosal, right and left anterior SLF (the SLF segment projecting between frontal and parietal cortex, Catani, Jones, & ffytche, 2005), and right and left arcuate fasciculus (the SLF long branch projecting between frontal and temporal cortex; Catani et al., 2005) microstructure of normal-hearing younger and older listeners. Next, we evaluated the degree to which individual differences in white matter microstructure predicted the ability of younger and older listeners to localize, attend, and identify a spoken digit stream while a competing digit stream was presented in a different location. Finally, we

examined whether individual differences in white matter microstructure accounted for age-group differences in the auditory spatial task. Hearing thresholds, processing speed, and attentional control were also considered as potential influences on auditory spatial processing.

6. Method

6.1. Participants

Participants included 47 adults (22 younger:19–30 years of age, 16 women; 25 older: 56–82 years of age, 18 women). Younger participants generally consisted of graduate student volunteers from the Medical University of South Carolina and undergraduate and graduate student volunteers from the College of Charleston, many of whom previously participated in hearing studies. Older participants consisted of volunteers from an ongoing longitudinal study on presbycusis and volunteers from the greater Charleston, SC community. Many participants, both younger and older, were familiar with laboratory testing but were unfamiliar with the tests employed in the current investigation. All participants were native English speakers with little to no cognitive impairment, having completed the Mini-Mental State Examination (Folstein et al., 1983) with no more than 3 errors. Handedness was determined using the Edinburgh Handedness Inventory (Oldfield, 1971). All but one younger and two older participants were right-handed. The three left-handed participants performed well within the range of the right-handed participants in all experimental tasks and were not found to exhibit any obvious cortical structural differences. This study was approved by the Institutional Review Board of the Medical University of South Carolina and all participants provided written informed consent prior to participation.

6.2. Audiometric thresholds

Pure-tone audiometric thresholds at conventional frequencies were tested using TDH-39 headphones connected to a Madsen Astera^2 clinical audiometer calibrated to appropriate American National Standards Institute (ANSI) specifications (ANSI, 2010). Because the purpose of the current investigation was to evaluate the degree to which age-group differences in auditory spatial processing are accounted for by variability in white matter microstructure, hearing loss was limited in older participants. All participants had audiometric thresholds less than or equal to 40 dB HL at conventional audiometric frequencies from 250 Hz to 4,000 Hz. All participants had interaural asymmetries less than or equal to 15 dB HL. Average audiometric thresholds for both ears are shown in Fig. 1.

6.3. Interaural time difference digit segregation task

Auditory spatial processing was evaluated behaviorally using a digit segregation task previously found to relate to low-level auditory spatial processing in the auditory nerve (Harris et al., 2017) and auditory brainstem (Bharadwaj et al., 2014) and is similar to auditory segregation tasks used to evaluate auditory spatial localization and selective attention (e.g., Falkenberg et al., 2011; Lewald et al., 2016; Oberfeld and Klöckner-Nowotny, 2016; Singh et al., 2008). The digits “one”, “two”, “three”, and “four” were spoken aloud by a female speaker and monotonized at 184 Hz (close to the natural pitch of the speaker). Participants were presented with two simultaneous sequences of three

randomly selected digits on each trial. The two sequences were differentially spatialized to the left and right of midline by varying their interaural time difference (ITD). Prior to presentation of the sequences, a target sequence was cued by an auditory noise cue presented at the same ITD as the target sequence and a light on a response box (either left or right). Target direction was randomized across trials and ITD was randomized at 100, 200, 300, 400, 800, or 1,200 μs. Each ITD was used 210 times. Following presentation of the digit-sequences, participants were asked to input the three digits from the target sequence into a response box in the order they were heard. Feedback was provided after each response. A green light indicated that all three digits were correctly identified in the correct order. A yellow light indicated that two digits were correctly identified in the correct order. A red light indicated that fewer than two digits were correctly identified. Serial recall (the number of target digits correctly identified sequentially) was averaged across trials for each ITD and served as our measure of auditory spatial processing. Testing was performed in a sound attenuated booth and stimuli were presented through ER 3C insert earphones at 70 dB SPL using custom MATLAB scripts, a Tucker-Davis Technologies RZ6 Auditory Processor, and a custom response box. All participants completed the digit segregation task.

6.4. Connections Test

The Connections Test was used to determine whether individual differences in processing speed and attentional control accounted for variability in auditory spatial processing. The Connections Test (Salthouse et al., 2000), a variant of the Trail Making Test (Reitan, 1958, 1992), involves connecting circled letters and/or numbers in alpha-numeric order. The characters are pseudo-randomly organized in 7x7 arrays on 8.5”x11” sheets of paper. Characters are organized such that sequential targets are located in adjacent locations so as to limit the motor requirements for the test (Salthouse et al., 2000). On each trial, participants were asked to draw connections between targets using a pen, making as many connections as possible within 20 s without making an error. This involves locating and identifying targets, determining the next target, and locating, identifying, and responding to the next sequential target. If an error was made, the participant was asked to correct the error before continuing. The simple forms of the test involve connecting letters or numbers. Scores are averaged across two trials connecting letters and two trials connecting numbers. The complex forms of the test involve connecting alternating numbers and letters in alpha-numeric order. Scores are averaged across two trials starting with a letter and two trials starting with a number. The complex forms engage the perceptuomotor skills required for the simple forms, but with the addition of switching between numbers and letters, engaging attentional control. The Connections Test is postulated to measure both perceptuomotor processing speed (simple forms) and attentional control (complex forms). Metrics for perceptuomotor processing speed and attentional control derived from the Connections test are strongly associated with scores on other perceptual processing speed and attentional control tasks (Salthouse et al., 2000; Salthouse, 2005, 2011). The simple test scores were regressed from the complex scores to create a residualized complex score that represented the attentional control demands of the complex test without the perceptuomotor demands of the simple and complex tests (e.g., Eckert et al., 2010; Salthouse et al., 2000). All but one younger and one older participant completed the Connections Test.

6.5. Quick Speech-in-Noise Test

While auditory spatial processing is important for detecting, locating, and selecting the speech of a target talker within a noisy environment, spatial information is often omitted or diminished in clinical assessments of speech audibility in noise. To evaluate the extent to which white matter microstructure accounted for variability in spatial processing of speech specifically, as opposed to general speech processing, our participants also completed the Quick Speech-in-Noise Test (QuickSIN). QuickSIN is employed in clinical settings to measure speech-in-noise audibility. Sentence stimuli are presented monaurally in multi-talker babble, providing no interaural spatial information. Speech-in-noise performance is quantified as a single metric of signal-to-noise ratio loss (SNR loss) (Niquette et al., 2001). SNR loss is determined by computing the average number of keywords (out of 5) correctly identified in each sentence at each SNR (25, 20, 15, 10, 5, and 0 dB SNR), summing the averages, and subtracting the sum from 30. Higher SNR loss indicates worse speech-in-noise identification. Testing was performed in a sound attenuated booth and stimuli were presented through TDH-39 headphones at 70 dB HL using a combination of an Onkyo Compact Disk Player and an Interacoustics Audio Traveler (AA222). 20 younger and 23 older participants completed the QuickSIN test. One older and one younger participant were removed from analyses for having SNR loss more than two standard deviations above and below the mean across age-groups, respectively.

6.6. Diffusion imaging

Tractography analyses were performed to examine the extent to which callosal white matter microstructure predicted auditory spatial processing and accounted for age-group differences in auditory spatial processing. Magnetic resonance imaging (MRI) was performed using a Siemens 3T Prisma^{fit} scanner equipped with a 32-channel head coil. First, T1-weighted images were acquired. Scan parameters: GRAPPA with acceleration factor = 3, TR = 5000 ms, TE = 2.98 ms, flip angle = 4°, 176 slices with a 256 x 256 matrix, slice thickness = 1.0 mm, and no slice gap. Next, diffusion imaging was acquired. Scan parameters: TR = 3100 ms, TE = 80 ms, flip angle = 90°, voxel size = 2.5 x 2.5 × 2.5 mm, 64 directions, FOV = 220 mm with 100% phase Fourier, and b-values = 0, 1000, 2000 s/mm^2. Diffusion tensor imaging (DTI) scalars of FA were calculated at b = 1000 s/mm^2.

Eddy current correction and tensor fitting was performed using FSL (Smith et al., 2004). Participants' diffusion images were coregistered to their native space T1 images using SPM 8 (Ashburner et al., 2013). Whole brain deterministic streamlines tractography was performed using Automatic Fiber Quantification (AFQ) and mrDiffusion (Yeatman et al., 2012). Streamlines were included if they met the default settings; angle <30°, FA > 0.2, and tract lengths between 50 and 250 mm. These criteria were used to improve fiber tracking accuracy by controlling for noise in the diffusion tensor data and regions where fiber orientations can be unclear when crossing fibers are present (Yeatman et al., 2012). The corpus callosum fiber group, SLF (anterior branch), and arcuate fasciculus (SLF long branch) fiber tracts were extracted from the whole brain streamlines. The callosum fiber group was created by selecting streamlines that passed through the corpus callosum. The right and left SLF fiber tracts were created by selecting streamlines that passed through waypoint regions of interest (ROIs) in the frontal cortex and in the parietal cortex in the right

and left hemisphere, respectively. The right and left arcuate fiber tracts were created by selecting streamlines that passed through waypoint ROIs in the frontal cortex and in the temporal cortex in the right and left hemisphere, respectively. Streamlines in a tract were excluded when they failed to meet the minimum angle, FA, and/or length values described above. Missing data occurred when the tract had too few streamlines. The callosal fiber group, right SLF, and left arcuate were defined and measured in all 47 participants. The left SLF was defined and measured in 46 participants (22 younger, 24 older) and the right arcuate fasciculus was defined and measured in 45 participants (21 younger, 24 older). Scalars for white matter microstructure – fractional anisotropy (FA) and mean diffusivity (MD) – were measured for the whole-brain white matter and the corpus callosum of each participant by averaging the FA and MD values across the streamlines that comprised each of these large fiber group. The streamlines that comprised the right and left SLF and the right and left arcuate were core-weighted and their FA and MD values were averaged across the length of each fiber tract for each participant. Representative examples of the callosal fiber group and arcuate and SLF tracts are provided in Figs. 2-4, respectively. FA is a measure of the degree to which diffusion is anisotropic and is often used as a general measure of microstructural integrity. MD is a measure of the net degree of fluid displacement typically associated with cellular membrane density and fluid viscosity. Generally, healthy white matter is characterized by higher FA and lower MD (Alexander et al., 2011; Feldman et al., 2010).

Post hoc analyses of different sections of the corpus callosum were accomplished by segmenting the callosal fiber group using AFQ's "AFQ_SegmentCallosum" function. The "AFQ_SegmentCallosum" function produces eight callosal fiber tracts using inclusive regions of interest that are located in the left and right orbitofrontal, pre-frontal, superior frontal, motor, superior parietal, posterior parietal, occipital, and temporal cortex. However, the default superior parietal tract includes projections between homologous somatosensory cortex, as well as the anterior portions of the superior and inferior parietal lobules. To improve specificity, this default superior parietal tract was split into two separate tracts, one that terminates in somatosensory area and one that terminates in the superior and inferior parietal lobules. These two new tracts are designated "somatosensory" and "superior parietal", respectively. The resulting nine callosal fiber tracts segment the corpus callosum into different interhemispheric tracts from anterior to posterior, allowing us to investigate whether the relationship we observed between callosal microstructure and auditory spatial processing varies depending on what area of the corpus callosum is examined. Fig. 2 color-codes the callosal fiber group to illustrate the different tracts mapped by AFQ. The average core-weighted FA and MD for each callosal tract was computed for each participant and used for analysis. Of our 47 participants, interhemispheric callosal tracts were defined and measured for the anterior frontal area of 47 (22 younger, 25 older), the superior frontal area of 46 (22 younger, 24 older), the motor area of 45 (22 younger, 23 older), the somatosensory area of 42 (21 younger, 21 older), the superior parietal area of 45 (22 younger, 23 older), the posterior parietal area of 46 (22 younger, 24 older), the occipital area of 47 (22 younger, 25 older), the temporal area of 46 (22 younger, 24 older), and the orbitofrontal region of 21 (12 younger, 9 older). Orbitofrontal tracts can be difficult to identify reliably because of

susceptibility artifacts common in this region for echo-planar sequences. As such, the orbitofrontal tract was not considered in our post-hoc analyses.

6.7. Experimental design and statistical analysis

First, to consider the covariance among our variables, ad hoc Pearson product-moment correlation analyses were conducted and reported in Table 1. Age-group was dummy coded such that younger participants were coded as zero and older participants were coded as one. To determine the extent to which the corpus callosum, SLF, and arcuate fasciculus related to ITD digit segregation after accounting for whole-brain white matter, partial correlations controlling for whole-brain white matter microstructure (the average FA and MD across the whole brain streamlines) were conducted between ITD digit segregation and these white matter structures.

Linear mixed-effects regression (LMER) (Bliese, 2013) models were then tested to determine the extent to which audiometric thresholds and white matter microstructure accounted for age-group differences in auditory spatial processing. LMER is commonly used to test hypothesis-driven relationships between predictor and outcome variables while accounting for cluster-level attributes (i.e., nested variables such as ITD). Like linear regression, the coefficients of each predictor in a LMER model represent the relationship between that predictor and the outcome variable after accounting for the variance in the outcome variable already explained by all other predictors in the model. For the current investigation, a theory-guided hierarchical approach was used to test separate hypothesis-driven models that examined the degree to which the relationship between ITD digit segregation and age-group was accounted for by audiometric thresholds and white matter microstructure after controlling for ITD. Model testing was accomplished by comparing the total amount of variance explained by a model with age-group as a predictor to the total amount of variance explained by a model with a predictor we hypothesized would account for the relationship between ITD digit segregation and age-group. If the addition of the predictor improved model fit (i.e. the model accounted for significantly more variance in ITD digit segregation) and the relationship between age-group and ITD digit segregation did not change, then that additional predictor accounted for variance in ITD digit segregation that is independent of the variance accounted for by age. However, if the addition of the predictor improved model fit and *changed* the relationship between age-group and ITD digit segregation, it suggests that the predictor accounted for (at least some) of the age-related variance in ITD digit segregation. If the addition of the predictor failed to improve model fit, then it was excluded from the model (e.g., Bates et al., 2015; Cohen et al., 2003; Dias et al., 2018; Gelman and Hill, 2007; Lewis, 2007).

Structural equation models (SEMs) were then constructed to test the degree to which callosal microstructure, right arcuate microstructure, and attentional control mediate age-group differences in ITD digit segregation. Similar to LMER, SEM is a valuable statistical tool for testing hypothesis-driven relationships between predictor and outcome variables. SEM has the added benefit of being able to test for mediation effects between predictor and outcome variables using path analysis. We evaluated the degree to which age-group differences in auditory spatial processing, a latent variable comprised of digit segregation

across the six spatial ITDs, was mediated by callosal and right arcuate microstructure and attentional control.

Finally, post-hoc analyses were conducted to determine whether the relationship we observed between callosal microstructure and ITD digit segregation was dependent on specific segments of the corpus callosum. The same SEM from above was tested by substituting the microstructure of the entire corpus callosum with the microstructure of each of the eight callosal tracts.

All statistical analyses were performed in R using the lme4 (Bates et al., 2015) and lavaan (Rosseel, 2012) packages. All significant descriptive correlation analyses involving ITD digit segregation shown in Table 1 were found to survive correction for inflated family-wise error using the Benjamini-Hochberg procedure. Partial correlations were performed to determine the extent to which significant white matter relationships with ITD digit segregation were resilient to controlling for whole brain white matter FA and MD variance and are also shown in Table 1.

7. Results

7.1. Age and diffusion metrics relate to ITD digit segregation

ITD digit segregation was significantly related to age-group and to corpus callosum FA and right arcuate FA after controlling for whole-brain white matter microstructure. Since perceptuomotor processing speed was not found to be related to ITD digit segregation and SNR loss was not found to be related to ITD digit segregation or age-group (Table 1), we did not include them in further analyses.

Apparent in Fig. 5 are trends suggesting that ITD digit segregation improved as ITD increased to about 400 μs but declined for the longer 800 μs and 1200 μs conditions. To determine whether these trends were significant, orthogonal linear and quadratic contrasts were fit to the ITDs. We then tested a LMER model with ITD digit segregation as the outcome variable and age-group, the linear ITD contrast, and the quadratic ITD contrast as fixed factors, and participant as a random factor. Age-group significantly predicted ITD digit segregation, $B = -0.141$ (SE = 0.046), $\beta = -0.399$ (SE = 0.131), $t(45) = -3.055$, $p = 0.004$. The linear contrast also significantly predicted ITD digit segregation, suggesting that digit segregation improved as ITD increased from 100 to 1200 μs, $B = 0.002$ (SE = 0.001), $\beta = 0.038$ (SE=.016), $t(233) = 2.402$, $p = 0.017$. The quadratic contrast was also a significant predictor, suggesting that digit segregation was best at intermediate ITDs, $B = 0.005$ (SE = 0.001), $\beta = 0.113$ (SE = 0.016), $t(233) = 7.223$, $p < 0.001$. The results are similar to those reported in classic studies finding that spatial perception of nonspeech sounds increases, peaks, and then declines as ITDs become larger (Blodgett et al., 1956; Klumpp and Eady, 1956).

Adding average audiometric thresholds for the left and right ears to this model failed to improve model fit, $\chi^2(1) = 0.041$, $p = 0.840$, and audiometric thresholds failed to account for a significant amount of the variability in ITD digit segregation accounted for by age-group. The following sections examine the extent to which age-group differences in ITD

digit segregation were accounted for by the corpus callosum FA and the right arcuate FA associations with ITD digit segregation.

7.2. Interhemispheric white matter fibers account for age-group differences in ITD digit segregation

Adding callosal FA as a predictor to the age-group model from above improved model fit, $\chi^2(1) = 4.152$, $p = 0.042$. ITD digit segregation continued to be predicted by the linear ITD contrast, $B = 0.002$ (SE = 0.001), $\beta = 0.038$ (SE = 0.016), $t(233) = 2.402$, $p = 0.017$, and quadratic ITD contrast, $B = 0.005$ (SE = 0.001), $\beta = 0.113$ (SE=.016), $t(233) = 7.223$, $p < 0.001$. Callosal FA also significantly predicted ITD digit segregation, $B = 1.543$ (SE = 0.765), $\beta = 0.296$ (SE = 0.147), $t(44) = 2.016$, $p = 0.050$. However, age-group no longer proved a significant predictor, $B = -.088$ (SE = 0.052), $\beta = -0.248$ (SE = 0.147), $t(44) = -1.690$, $p = 0.098$. The results suggest that age-group differences in ITD digit segregation may be accounted for by individual differences in callosal FA. The interaction between age-group and callosal FA failed to improve model fit, $\chi^2(1) = 0.361$, $p = 0.548$, and did not significantly predict ITD digit segregation. This result demonstrates that callosal FA and ITD digit segregation did not exhibit different patterns of covariance in older and younger adults, as shown in Fig. 6 where the relationship between callosal FA and ITD digit segregation is presented.

7.3. Intrahemispheric white matter fibers account for age-independent differences in ITD digit segregation

The age-group model from above was retested on the subset of 45 participants with measured right arcuate microstructure. ITD digit segregation was significantly predicted by age-group, $B = -0.138$ (SE = 0.048), $\beta = -0.385$ (SE = 0.135), $t(43) = -2.860$, $p = 0.007$, the linear ITD contrast, $B = 0.002$ (SE = 0.001), $\beta = 0.033$ (SE=.016), $t(223) = 2.092$, $p = 0.038$, and the quadratic ITD contrast, $B = 0.005$ (SE = 0.001), $\beta = 0.111$ (SE = 0.016), $t(223) = 6.969$, $p < 0.001$. Adding right arcuate FA as a predictor to this model improved model fit, $\chi^2(1) = 9.483$, $p = 0.002$. ITD digit segregation continued to be predicted by age-group, $B = -0.130$ (SE = 0.044), $\beta = -0.365$ (SE = 0.123), $t(42) = -2.968$, $p = 0.005$, the linear ITD contrast, $B = 0.002$ (SE = 0.001), $\beta = 0.033$ (SE = 0.016), $t(223) = 2.092$, $p = 0.038$, and the quadratic ITD contrast, $B = 0.005$ (SE = 0.001), $\beta = 0.111$ (SE=.016), $t(223) = 6.969$, $p < 0.001$. Right arcuate FA also significantly predicted ITD digit segregation, $B = 1.303$ (SE = 0.415), $\beta = 0.386$ (SE = 0.123), $t(42) = 3.139$, $p = 0.003$. The results suggest that age-group differences in ITD digit segregation were not accounted for by individual differences in right arcuate FA, but right arcuate FA independently accounted for variability in ITD digit segregation. Adding an interaction term for age-group and right arcuate FA also failed to improve model fit, $\chi^2(1) = 0.181$, $p = 0.671$, suggesting the relationship between right arcuate FA and ITD digit segregation was not significantly different between age-groups. The relationship between right arcuate FA and ITD digit segregation is represented in Fig. 7.

7.4. SEM for age-related and normative variation in ITD digit segregation

The interhemispheric LMER models from above found that individual differences in callosal FA accounted for the variance in ITD digit segregation explained by age-group, suggesting that callosal FA could have mediated age-group differences in ITD digit segregation. The

intrahemispheric LMER models from above found that individual differences in right arcuate FA accounted for variability in ITD digit segregation independent of age-group, suggesting a normative individual difference effect. An SEM model was constructed to determine the degree to which callosal FA and right arcuate FA independently predict and mediated age-group differences in ITD digit segregation. The SEM model is reported in Fig. 8A. The parameter estimates for the full model are reported in Table 2. Age-group predicted callosal FA and callosal FA predicted ITD digit segregation. Age-group did not predict right arcuate FA, but as shown earlier, right arcuate FA predicted ITD digit segregation. The SEM results suggest that right arcuate FA and Callosal FA independently predicted ITD digit segregation, but only callosal FA mediated age-group differences in ITD digit segregation.

Interestingly, attentional control was found to relate to both ITD digit segregation and right arcuate FA, but was unrelated to age-group (Table 1). This pattern of relationships may suggest that attentional control plays a role in the relationship between right arcuate FA and ITD digit segregation. The SEM model was updated to incorporate these relationships, depicted in Fig. 8B. The model fit and parameter estimates for the full model are reported in Table 3. Overall model fit did not significantly change, $\chi^2(8) = 1.167$, $p = 0.997$.

In summary, the SEMs suggest that individual differences in callosal microstructure and right arcuate microstructure have independent roles in ITD digit segregation. Individual differences in callosal microstructure may mediate age-group differences in ITD digit segregation and attentional control may play a role in the relationship between right arcuate microstructure and ITD digit segregation (Fig. 9).

7.5. Post-hoc analyses

As described above, different callosal fibers projecting from different sections of the corpus callosum were mapped and measured using AFQ's "AFQ_SegmentCallosum" function. Reported in Table 4, age-group was negatively associated with the FA of each of the callosal tracts with the only exception being the callosal tract connecting left and right temporal lobe. These significant relationships survived correction for inflated family-wise error using the Benjamini-Hochberg procedure. The FA values for each of these tracts substituted the callosal FA values in separate SEMs based on the model in Fig. 8A to determine which of these callosal tracts predicted ITD digit segregation and mediated age-group differences after accounting for right arcuate FA. A summary of the parameter estimates for the structural model of each tract are reported in Table 5. The only callosal tracts found to be significant predictors of ITD digit segregation and mediated age-group differences in ITD digit segregation after accounting for right arcuate microstructure were the callosal tracts connecting left and right pre-frontal cortex and left and right posterior parietal lobe.

8. Discussion

Higher callosal FA predicted better ITD digit segregation in younger and older listeners. The results build upon studies finding the corpus callosum and the interhemispheric communication of auditory spatial information important for auditory spatial perception (Hausmann et al., 2005; Lepore et al., 2002; Poirier et al., 1993, 1995; Rock and Apicella, 2015). Higher, right arcuate FA also predicted better ITD digit segregation in younger and

older adults, consistent with the hypothesized role of the right arcuate fasciculus in auditory spatial attention (Barrick et al., 2006). Importantly, callosal and right arcuate FA accounted for independent variance in ITD digit segregation, suggesting that individual differences in interhemispheric and intrahemispheric white matter microstructure contribute to variability in auditory spatial processing.

8.1. Interhemispheric white matter accounts for age-group differences in auditory spatial processing

Older listeners were found to have lower callosal FA and individual differences in callosal FA were found to mediate age-related deficits in ITD digit segregation. Our post-hoc SEMs suggested that the relationship between callosal microstructure and ITD digit segregation varies depending on which callosal fibers are concerned. Age-related declines in callosal microstructure may degrade spatial information communicated across hemispheres and negatively impact auditory spatial processing. The results provide structural support for findings suggesting interhemispheric processing is important for auditory spatial perception (e.g., Grady et al., 2011; Greenwald and Jerger, 2001; Lewald et al., 2016; Rauschecker, 2018). The results also provide a cortical mechanism to account for age-related deficits in auditory spatial processing (Freigang et al., 2015; Freigang et al., 2014; Gallun et al., 2009; Greenwald and Jerger, 2001; Hawkins and Wightman, 1980; Smoski and Trahiotis, 1986).

Age-group differences in FA across callosal tracts suggests that the callosal results are not due to a differential pattern of aging in the fibers passing through the genu and splenium compared to the body of the corpus callosum. Instead, the results suggest a more specific mapping of callosal projections between cortical structures that support auditory spatial processing. The differentiation in the callosal tracts that are important for spatial processing suggests that the interhemispheric integration of auditory spatial information is accomplished in specific cortical structures. Pre-frontal cortex integrates auditory (and visual) spatial information with working memory, attention, and sensorimotor mechanisms to guide behavior (Bushara et al., 1999; Lewald et al., 2008; Rauschecker, 2018), while posterior parietal cortex represents spatial information relative to body position (Cohen et al., 2005; Lewald et al., 2002; Lewald et al., 2004). These broad cortical areas may be important sites for integrating intrahemispheric spatial information transmitted across the corpus callosum.

Temporal lobe projections of the corpus callosum were not significantly associated with ITD digit segregation. This negative result may indicate that some aspects of auditory spatial processing are performed with direct input from the auditory nerve (Harris et al., 2017) and auditory brainstem (Bharadwaj et al., 2014, 2015) before information is integrated across hemispheres via the corpus callosum. In addition, callosal fibers projecting to the temporal lobe must tangentially cross other major fiber bundles, which negatively affects fiber tracking and diffusion metrics (Jarbo et al., 2012), and thus diminishes sensitivity for characterizing individual differences in ITD digit segregation. This premise is supported by the absence of an age-group association with the temporally projecting callosum fibers.

8.2. Attentional control reflects the role of the right arcuate in auditory spatial processing

Attentional control, as measured using the Connections Test, also predicted ITD digit segregation. This is not unusual considering the attentional demands of the task, which require a listener to localize and attend to a spoken digit stream in one location while a competing digit stream is spoken in another location. Similar to right arcuate FA, attentional control was unrelated to age-group and did not mediate age-group differences in ITD digit segregation. However, attentional control was related to right arcuate FA. Our SEM (Fig. 8B) demonstrated that attentional control can mediate the role of arcuate FA in ITD digit segregation. The relationships are consistent with the hypothesized role of the right arcuate in spatial attention (Barrick et al., 2006) and the attentional demands of the ITD digit segregation task.

8.3. Additional caveats

Evidence largely coming from stroke patients with visual spatial neglect suggests that the SLF is important for visual spatial attention (e.g., Carter et al., 2017; Chechlacz et al., 2010; Chechlacz et al., 2013; Karnath and Rorden, 2012; Karnath et al., 2009; Meola et al., 2015; Molenberghs et al., 2012; Suchan et al., 2014; Thiebaut de Schotten et al., 2012; Urbanski et al., 2011; Vaessen et al., 2016). The current investigation found that the long branch of the SLF, the arcuate fasciculus, was related to ITD digit segregation, but the anterior portion of the SLF was not. The failure of the anterior SLF to predict ITD digit segregation may be due to the susceptibility of fiber tracts to noise resulting from crossing fibers and pruning errors, which can affect measurements of FA (Beaulieu, 2002; Jones et al., 2013; Mädler et al., 2008). Alternatively, the failure of the anterior SLF to predict ITD digit segregation may suggest that the relationship between the SLF and auditory spatial attention is specific to fibers terminating in the frontal and temporal cortices. This differentiation is relevant for determining which SLF fibers are important for auditory and visual spatial attention. The results may also be important for better understanding the underlying neural pathology associated with auditory and visual attentional neglect.

It may be surprising that SNR loss did not relate to age-group. However, this is consistent with other studies examining QuickSIN performance among groups of older listeners that are high-functioning and have limited hearing loss (e.g., McClaskey et al., 2019; Sheft et al., 2012). More interesting is the lack of a relationship between SNR loss and ITD digit segregation, which may suggest that the subtle individual differences in speech-in-noise identification among normal hearing younger and older listeners as measured by QuickSIN are not sensitive enough to account for variability in ITD digit segregation. Alternatively, the lack of a relationship may suggest that the ability to identify speech in noise is largely unrelated to the ability to localize, attend, and identify spatially cued speech. Future studies should use more sensitive measures of speech-in-noise identification to better elucidate the degree to which speech-in-noise performance plays a role in auditory spatial attention.

9. Conclusion

The ability to detect, locate, and select a talker from among others is important for effectively communicating in noisy listening environments. Age-related deficits in the

peripheral and central nervous system can have detrimental effects on the capacity to use auditory spatial information to successfully communicate within such “cocktail party” scenarios. Much of the extant literature focuses on the capacity of older adults to identify speech within the noise of such environments, with little regard for other factors that contribute to effective speech communication, including auditory spatial processing (auditory spatial localization and attention). The results of the current investigation suggest that individual differences in callosal and right arcuate microstructure are important for selecting and identifying the speech of one talker from another spatially discriminant talker. The corpus callosum may facilitate interhemispheric integration of information important for auditory spatial processing. Further, age-related deficits in callosal microstructure may degrade auditory spatial information communicated across hemispheres, negatively impacting sound localization and attention and perhaps contributing to the difficulties older listeners have communicating in complex listening environments.

Acknowledgements

This work was supported (in part) by grants from the National Institute on Deafness and Other Communication Disorders (NIDCD) (R01 DC014467, R01 DC017619, P50 DC00422, and T32 DC014435). The project also received support from the South Carolina Clinical and Translational Research (SCTR) Institute with an academic home at the Medical University of South Carolina, National Institute of Health/National Center for Research Resources (NIH/NCRR) Grant number UL1RR029882. This investigation was conducted in a facility constructed with support from Research Facilities Improvement Program Grant Number C06 RR1 4516 from the National Center for Research Resources, NIH. The authors declare no competing financial interests.

References

Alexander AL, Hurley SA, Samsonov AA, Adluru N, Hosseinbor AP, Mossahebi P, et al., 2011 Characterization of cerebral white matter properties using quantitative magnetic resonance imaging stains. Brain Connect. 1 (6), 423–446. 10.1089/brain.2011.0071. [PubMed: 22432902]

ANSI, 2010 Specification for Audiometrics. American National Standards Institute, New York.

Ashburner J, Barnes G, Chen C-C, Daunizeau J, Flandin G, Friston K, et al., 2013 SPM8 Manual Functional Imaging Laboratory, Welcome Trust Centre of Neuroimaging, Institute of Neurology, UCL, London, UK.

Barrick TR, Lawes IN, Mackay CE, Clark CA, 2006 White matter pathway asymmetry underlies functional lateralization. Cerebr. Cortex 17 (3), 591–598. 10.1093/cercor/bhk004.

Bates D, Mächler M, Bolker B, Walker S, 2015 Fitting linear mixed-effects models using lme4, 67 (1), 48 10.18637/jss.v067.i01.

Beaulieu C, 2002 The basis of anisotropic water diffusion in the nervous system – a technical review. NMR Biomed. 15 (7-8), 435–455. 10.1002/nbm.782. [PubMed: 12489094]

Bharadwaj H, Verhulst S, Shaheen L, Liberman MC, Shinn-Cunningham B, 2014 Cochlear neuropathy and the coding of supra-threshold sound. Front. Syst. Neurosci 8 (26) 10.3389/fnsys.2014.00026.

Bharadwaj HM, Masud S, Mehraei G, Verhulst S, Shinn-Cunningham BG, 2015 Individual differences reveal correlates of hidden hearing deficits. J. Neurosci 35 (5), 2161–2172. 10.1523/jneurosci.3915-14.2015. [PubMed: 25653371]

Bliese P, 2013 Multilevel Models in R (2.5): A Brief Introduction to R, the Multilevel Package and the Nlme Package.

Blodgett HC, Wilbanks WA, Jeffress LA, 1956 Effect of large interaural time differences upon the judgment of sidedness. J. Acoust. Soc. Am 28 (4), 639–643. 10.1121/1.1908430.

Bushara KO, Weeks RA, Ishii K, Catalan M-J, Tian B, Rauschecker JP, Hallett M, 1999 Modality-specific frontal and parietal areas for auditory and visual spatial localization in humans. Nat. Neurosci 2, 759 10.1038/11239. [PubMed: 10412067]

Carter AR, McAvoy MP, Siegel JS, Hong X, Astafiev SV, Rengachary J, et al., 2017 Differential white matter involvement associated with distinct visuospatial deficits after right hemisphere stroke. Cortex 88, 81–97. 10.1016/j.cortex.2016.12.009. [PubMed: 28081452]

Catani M, Jones DK, ffytche DH, 2005 Perisylvian language networks of the human brain. Ann. Neurol 57 (1), 8–16. 10.1002/ana.20319. [PubMed: 15597383]

Chechlacz M, Rotshtein P, Bickerton W-L, Hansen PC, Deb S, Humphreys GW, 2010 Separating neural correlates of allocentric and egocentric neglect: distinct cortical sites and common white matter disconnections. Cogn. Neuropsychol 27 (3), 277–303. 10.1080/02643294.2010.519699. [PubMed: 21058077]

Chechlacz M, Rotshtein P, Hansen PC, Deb S, Riddoch MJ, Humphreys GW, 2013 The central role of the temporo-parietal junction and the superior longitudinal fasciculus in supporting multi-item competition: evidence from lesion-symptom mapping of extinction. Cortex 49 (2), 487–506. 10.1016/j.cortex.2011.11.008. [PubMed: 22192727]

Cohen J, Cohen P, West SG, Aiken LS, 2003 Applied Multiple Regression/Correlation Analysis for the Behavioral Sciences. Lawrency Erlbaum Associates, Mahwah, NJ.

Cohen YE, Russ BE, Gifford GW, 2005 Auditory processing in the posterior parietal cortex. Behav. Cognit. Neurosci. Rev 4 (3), 218–231. 10.1177/1534582305285861. [PubMed: 16510894]

Dias JW, McClaskey CM, Harris KC, 2018 Time-compressed speech identification is predicted by auditory neural processing, perceptuomotor speed, and executive functioning in younger and older listeners. JARO J. Assoc. Res. Otolaryngol 10.1007/s10162-018-00703-1.

Dubno JR, Dirks DD, Morgan DE, 1984 Effects of age and mild hearing loss on speech recognition in noise. J. Acoust. Soc. Am 76 (1), 87–96. 10.1121/1.391011. [PubMed: 6747116]

Eckert M, Keren N, Roberts D, Calhoun V, Harris K, 2010 Age-related changes in processing speed: unique contributions of cerebellar and prefrontal cortex. Front. Hum. Neurosci 4 (10) 10.3389/neuro.09.010.2010.

Falkenberg LE, Specht K, Westerhausen R, 2011 Attention and cognitive control networks assessed in a dichotic listening fMRI study. Brain Cognit. 76 (2), 276–285. 10.1016/j.bandc.2011.02.006. [PubMed: 21398015]

Feldman HM, Yeatman JD, Lee ES, Barde LHF, Gaman-Bean S, 2010 Diffusion tensor imaging: a review for pediatric researchers and clinicians. J. Dev. Behav. Pediatr. : JDBP (J. Dev. Behav. Pediatr.) 31 (4), 346–356. 10.1097/DBP.0b013e3181dcaa8b. [PubMed: 20453582]

Folstein MF, Robins LN, Helzer JE, 1983 The mini-mental state examination. Arch. Gen. Psychiatr 40 (7), 812 10.1001/archpsyc.1983.01790060110016. [PubMed: 6860082]

Freigang C, Schmiedchen K, Nitsche I, Rübsamen R, 2014 Free-field study on auditory localization and discrimination performance in older adults. Exp. Brain Res 232 (4), 1157–1172. 10.1007/s00221-014-3825-0. [PubMed: 24449009]

Freigang C, Richter N, Rübsamen R, Ludwig AA, 2015 Age-related changes in sound localisation ability. Cell Tissue Res. 361 (1), 371–386. 10.1007/s00441-015-2230-8. [PubMed: 26077928]

Füllgrabe C, Moore BCJ, Stone MA, 2015 Age-group differences in speech identification despite matched audiometrically normal hearing: contributions from auditory temporal processing and cognition. Front. Aging Neurosci 6 (347) 10.3389/fnagi.2014.00347.

Gallun FJ, Diedesch A, Engelking E, 2009 The impacts of age and absolute threshold on binaural lateralization. Proc. Meet. Acoust 6 (1), 050005 10.1121/1.3274791.

Gelman A, Hill J, 2007 Data Analysis Using Regression and Mutlilevel/Heirarchical Models. Cambridge University Press, New York, NY.

Grady CL, Alain C, Yu H, 2007 Age-related differences in brain activity underlying working memory for spatial and nonspatial auditory information. Cerebr. Cortex 18 (1), 189–199. 10.1093/cercor/bhm045.

Grady C, Charlton R, Yu H, Alain C, 2011 Age differences in fMRI adaptation for sound identity and location. Front. Hum. Neurosci 5 (24) 10.3389/fnhum.2011.00024.

Greenwald RR, Jerger J, 2001 Aging affects hemispheric asymmetry on a competing speech task. J. Am. Acad. Audiol 12 (4), 167–173. [PubMed: 11332516]

Griffiths TD, Rees G, Rees A, Green GGR, Witton C, Rowe D, et al., 1998 Right parietal cortex is involved in the perception of sound movement in humans. Nat. Neurosci 1 (1), 74–79. 10.1038/276. [PubMed: 10195113]

Griffiths TD, Green GGR, Rees A, Rees G, 2000 Human brain areas involved in the analysis of auditory movement. Hum. Brain Mapp 9 (2), 72–80. 10.1002/(sici)1097-0193(200002)9:2<72::Aid-hbm2>3.0.Co;2-9. [PubMed: 10680764]

Harris CS, Vaden KI, McClaskey CM, Dias JW, Dubno JR, 2017 Complementary metrics of human auditory nerve function derived from compound action potentials. J. Neurophysiol 119, 1019–1028. 10.1152/jn.00638.2017. [PubMed: 29187555]

Hausmann M, Corballis MC, Fabri M, Paggi A, Lewald J, 2005 Sound lateralization in subjects with callosotomy, callosal agenesis, or hemispherectomy. Cognit. Brain Res 25 (2), 537–546. 10.1016/j.cogbrainres.2005.08.008.

Hawkins DB, Wightman FL, 1980 Interaural time discrimination ability of listeners with sensorineural hearing loss. Audiology 19 (6), 495–507. 10.3109/00206098009070081. [PubMed: 7425954]

Huang S, Chang W-T, Belliveau JW, Hämäläinen M, Ahveninen J, 2014 Lateralized parietotemporal oscillatory phase synchronization during auditory selective attention. Neuroimage 86, 461–469. 10.1016/j.neuroimage.2013.10.043. [PubMed: 24185023]

Jarbo K, Verstynen T, Schneider W, 2012 In vivo quantification of global connectivity in the human corpus callosum. Neuroimage 59 (3), 1988–1996. 10.1016/j.neuroimage.2011.09.056. [PubMed: 21985906]

Jones DK, Knösche TR, Turner R, 2013 White matter integrity, fiber count, and other fallacies: the do's and don'ts of diffusion MRI. Neuroimage 73, 239–254. 10.1016/j.neuroimage.2012.06.081. [PubMed: 22846632]

Karnath H-O, Rorden C, 2012 The anatomy of spatial neglect. Neuropsychologia 50 (6), 1010–1017. 10.1016/j.neuropsychologia.2011.06.027. [PubMed: 21756924]

Karnath H-O, Rorden C, Ticini LF, 2009 Damage to white matter fiber tracts in acute spatial neglect. Cerebr. Cortex 19 (10), 2331–2337. 10.1093/cercor/bhn250.

Klumpp RG, Eady HR, 1956 Some measurements of interaural time difference thresholds. J. Acoust. Soc. Am. 28 (5), 859–860. 10.1121/1.1908493.

Lepore F, Villemagne J, Lassonde M, Lessard N, 2002 Sound localization in callosal agenesis and early callosotomy subjects: brain reorganization and/or compensatory strategies. Brain 125 (5), 1039–1053. 10.1093/brain/awf096. [PubMed: 11960894]

Lewald J, Foltys H, Töpper R, 2002 Role of the posterior parietal cortex in spatial hearing. J. Neurosci 22 (3), RC207 10.1523/jneurosci.22-03-j0005.2002. [PubMed: 11826153]

Lewald J, Wienemann M, Boroojerdi B, 2004 Shift in sound localization induced by rTMS of the posterior parietal lobe. Neuropsychologia 42 (12), 1598–1607. 10.1016/j.neuropsychologia.2004.04.012. [PubMed: 15327928]

Lewald J, Riederer KAJ, Lentz T, Meister IG, 2008 Processing of sound location in human cortex. Eur. J. Neurosci 27 (5), 1261–1270. 10.1111/j.1460-9568.2008.06094.x. [PubMed: 18364040]

Lewald J, Hanenberg C, Getzmann S, 2016 Brain correlates of the orientation of auditory spatial attention onto speaker location in a "cocktail-party" situation. Psychophysiology 53 (10), 1484–1495. 10.1111/psyp.12692. [PubMed: 27333881]

Lewis ME, 2007 Stepwise versus Hierarchical Regression: Pros and Cons. Paper presented at the Annual Meeting of the Southwest Educational Research Association, San Antonio.

Mädler B, Drabycz SA, Kolind SH, Whittall KP, MacKay AL, 2008 Is diffusion anisotropy an accurate monitor of myelination?: correlation of multicomponent T2 relaxation and diffusion tensor anisotropy in human brain. Magn. Reson. Imag 26 (7), 874–888. 10.1016/j.mri.2008.01.047.

McClaskey CM, Dias JW, Harris KC, 2019 Sustained envelope periodicity representations are associated with speech-in-noise performance in difficult listening conditions for younger and older adults. J. Neurophysiol 10.1152/jn.00845.2018, 0(0), null.

Meola A, Comert A, Yeh F-C, Stefaneanu L, Fernandez-Miranda JC, 2015 The controversial existence of the human superior fronto-occipital fasciculus: connectome-based tractographic study with microdissection validation. Hum. Brain Mapp 36 (12), 4964–4971. 10.1002/hbm.22990. [PubMed: 26435158]

Molenberghs P, Sale M, Mattingley J, 2012 Is there a critical lesion site for unilateral spatial neglect? A meta-analysis using activation likelihood estimation. Front. Hum. Neurosci 6 (78) 10.3389/fnhum.2012.00078.

Niquette P, Gudmundsen G, Killion M, 2001 QuickSIN Speech-In-Noise Test Version 1.3. Etymotic Research, Elk Grove Village, IL.

Nusbaum AO, Tang CY, Buchsbaum MS, Wei TC, Atlas SW, 2001 Regional and global changes in cerebral diffusion with normal aging. Am. J. Neuroradiol 22 (1), 136–142. [PubMed: 11158899]

Oberfeld D, Klöckner-Nowotny F, 2016 Individual differences in selective attention predict speech identification at a cocktail party. eLife 5, e16747 10.7554/eLife.16747. [PubMed: 27580272]

Oldfield RC, 1971 The assessment and analysis of handedness: the Edinburgh inventory. Neuropsychologia 9 (1), 97–113. 10.1016/0028-3932(71)90067-4. [PubMed: 5146491]

Ota M, Obata T, Akine Y, Ito H, Ikehira H, Asada T, Suhara T, 2006 Age-related degeneration of corpus callosum measured with diffusion tensor imaging. Neuroimage 31 (4), 1445–1452. 10.1016/j.neuroimage.2006.02.008. [PubMed: 16563802]

Pfefferbaum A, Sullivan EV, Carmelli D, 2004 Morphological changes in aging brain structures are differentially affected by time-linked environmental influences despite strong genetic stability. Neurobiol. Aging 25 (2), 175–183. 10.1016/S0197-4580(03)00045-9. [PubMed: 14749135]

Poirier P, Miljours S, Lassonde M, Lepore F, 1993 Sound localization in acallosal human listeners. Brain 116 (1), 53–69. 10.1093/brain/116.1.53. [PubMed: 8453465]

Poirier P, Lepore F, Provençal C, Ptito M, Guillemot J-P, 1995 Binaural noise stimulation of auditory callosal fibers of the cat: responses to interaural time delays. Exp. Brain Res 104 (1), 30–40. 10.1007/bf00229853. [PubMed: 7621939]

Rauschecker JP, 2018 Where, When, and How: are they all sensorimotor? Towards a unified view of the dorsal pathway in vision and audition. Cortex 98, 262–268. 10.1016/j.cortex.2017.10.020. [PubMed: 29183630]

Reitan RM, 1958 Validity of the trail making test as an indicator of organic brain damage. Percept. Mot. Skills 8 (3), 271–276. 10.2466/pms.1958.8.3.271.

Reitan RM, 1992 Trail Making Test: Manual for Administration and Scoring [adults]. Reitan Neuropsychology Laboratory, Tucson, Ariz.

Rock C, Apicella A.j., 2015 Callosal projections drive neuronal-specific responses in the mouse auditory cortex. J. Neurosci 35 (17), 6703–6713. 10.1523/jneurosci.5049-14.2015. [PubMed: 25926449]

Rosseel Y, 2012 lavaan: An R package for structural equation modeling, 48 (2), 36 10.18637/jss.v048.i02, 2012.

Salat DH, Tuch DS, Greve DN, van der Kouwe AJW, Hevelone ND, Zaleta AK, et al., 2005 Age-related alterations in white matter microstructure measured by diffusion tensor imaging. Neurobiol. Aging 26 (8), 1215–1227. 10.1016/j.neurobiolaging.2004.09.017. [PubMed: 15917106]

Salthouse TA, 2005 Relations between cognitive abilities and measures of executive functioning. Neuropsychology 19 (4), 532–545. 10.1037/0894-4105.19.4.532. [PubMed: 16060828]

Salthouse TA, 2011 What cognitive abilities are involved in trail-making performance? Intelligence 39 (4), 222–232. 10.1016/j.intell.2011.03.001. [PubMed: 21789028]

Salthouse TA, Toth J, Daniels K, Parks C, Pak R, Wolbrette M, Hocking KJ, 2000 Effects of aging on efficiency of task switching in a variant of the Trail Making Test. Neuropsychology 14 (1), 102–111. 10.1037/0894-4105.14.1.102. [PubMed: 10674802]

Sheft S, Shafiro V, Lorenzi C, McMullen R, Farrell C, 2012 Effects of age and hearing loss on the relationship between discrimination of stochastic frequency modulation and speech perception. Ear Hear. 33 (6), 709–720. 10.1097/AUD.0b013e31825aab15. [PubMed: 22790319]

Singh G, Pichora-Fuller MK, Schneider BA, 2008 The effect of age on auditory spatial attention in conditions of real and simulated spatial separation. J. Acoust. Soc. Am 124 (2), 1294–1305. 10.1121/1.2949399. [PubMed: 18681615]

Smith SM, Jenkinson M, Woolrich MW, Beckmann CF, Behrens TEJ, Johansen-Berg H, et al., 2004 Advances in functional and structural MR image analysis and implementation as FSL. Neuroimage 23, S208–S219. 10.1016/j.neuroimage.2004.07.051. [PubMed: 15501092]

Smoski WJ, Trahiotis C, 1986 Discrimination of interaural temporal disparities by normal-hearing listeners and listeners with high-frequency sensorineural hearing loss. J. Acoust. Soc. Am 79 (5), 1541–1547. 10.1121/1.393680. [PubMed: 3711453]

Suchan J, Umarova R, Schnell S, Himmelbach M, Weiller C, Karnath H-O, Saur D, 2014 Fiber pathways connecting cortical areas relevant for spatial orienting and exploration. Hum. Brain Mapp 35 (3), 1031–1043. 10.1002/hbm.22232. [PubMed: 23283834]

Teubner-Rhodes S, Vaden KI, Cute SL, Yeatman JD, Dougherty RF, Eckert MA, 2016 Aging-resilient associations between the arcuate fasciculus and vocabulary knowledge: microstructure or morphology? J. Neurosci 36 (27), 7210–7222. 10.1523/JNEUROSCI.4342-15.2016. [PubMed: 27383595]

Thiebaut de Schotten M, Tomaiuolo F, Aiello M, Merola S, Silvetti M, Lecce F, Doricchi F, 2012 Damage to white matter pathways in subacute and chronic spatial neglect: a group study and 2 single-case studies with complete virtual “in vivo” tractography dissection. Cerebr. Cortex 24 (3), 691–706. 10.1093/cercor/bhs351.

Urbanski M, Thiebaut de Schotten M, Rodrigo S, Oppenheim C, Touzé E, Méder J-F, et al., 2011 DTI-MR tractography of white matter damage in stroke patients with neglect. Exp. Brain Res 208 (4), 491–505. 10.1007/s00221-010-2496-8. [PubMed: 21113581]

Vaessen MJ, Saj A, Lovblad K-O, Gschwind M, Vuilleumier P, 2016 Structural white-matter connections mediating distinct behavioral components of spatial neglect in right brain-damaged patients. Cortex 77, 54–68. 10.1016/j.cortex.2015.12.008. [PubMed: 26922504]

Yeatman JD, Dougherty RF, Myall NJ, Wandell BA, Feldman HM, 2012 Tract profiles of white matter properties: automating fiber-tract quantification. PloS One 7 (11), e49790 10.1371/journal.pone.0049790. [PubMed: 23166771]

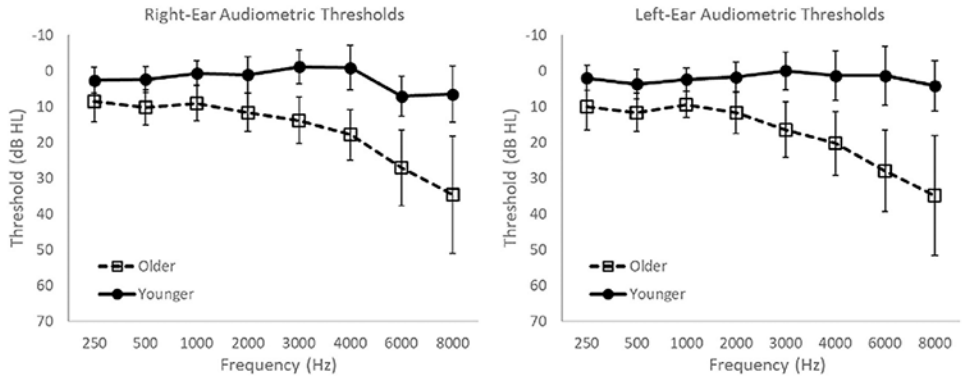

Fig. 1.

Audiometric thresholds of younger and older participants. Open squares indicate older listeners and filed circles indicate younger listeners. Error bars indicate 95% confidence intervals.

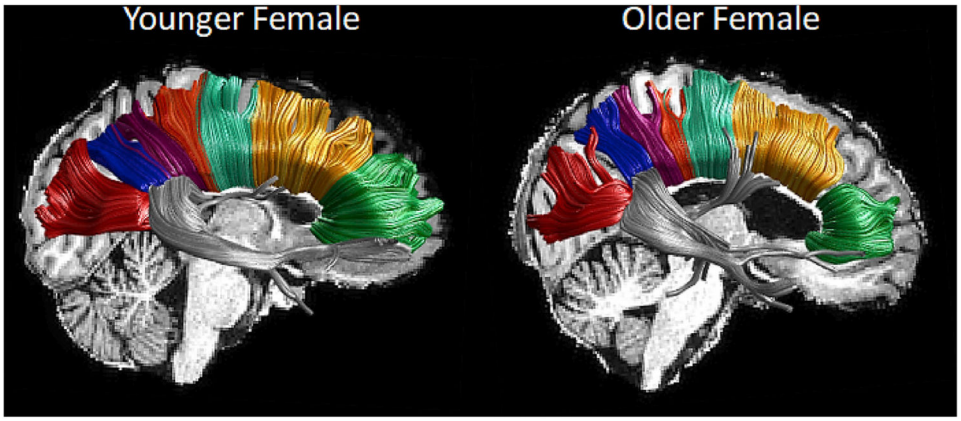

Fig. 2.

Tract renderings of the callosal fiber group and the fiber tracks mapped and quantified by AFQ_SegmentCallosum in a younger (left) 27 yo female participant with good ITD digit segregation and an older (right) 68 yo female participant with poor ITD digit segregation. Anterior to posterior: green = anterior frontal, gold = superior frontal, turquoise = motor, orange = somatosensory, violet = superior parietal, blue = posterior parietal, red = occipital, silver = temporal.

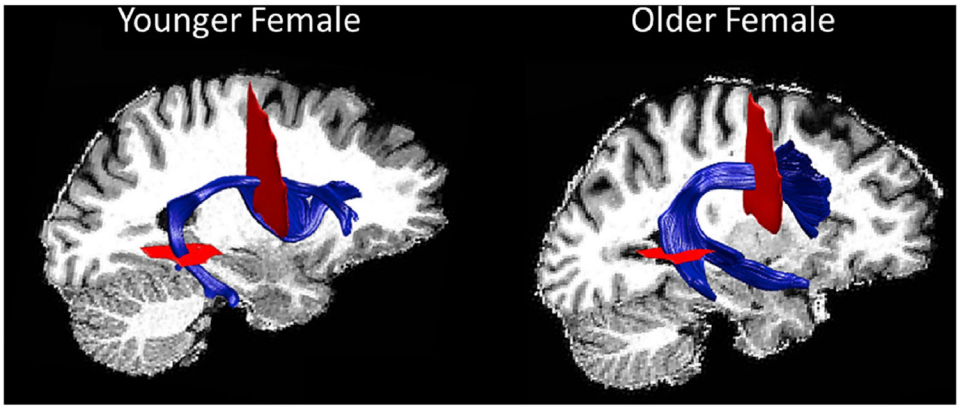

Fig. 3.

Tract renderings of the right arcuate fasciculus with corresponding waypoint regions of interest in a younger (left) 27 yo female participant with good ITD digit segregation and an older (right) 68 yo female participant with poor ITD digit segregation.

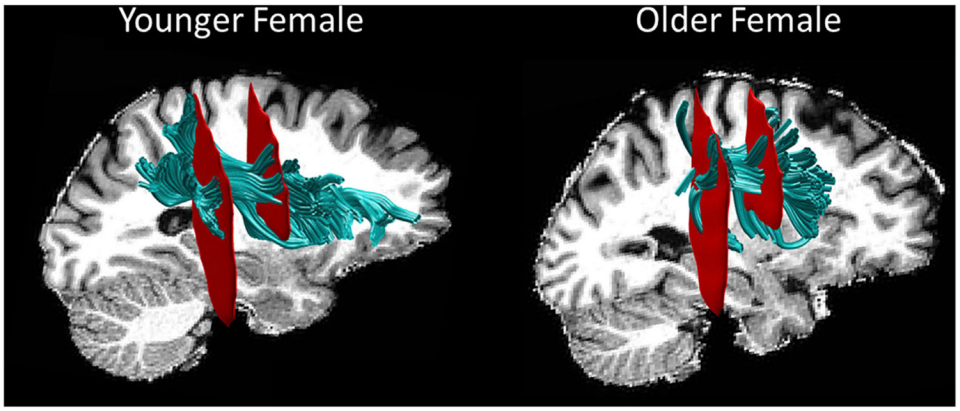

Fig. 4.

Tract renderings of the right superior longitudinal fasciculus (SLF) with corresponding waypoint regions of interest in a younger (left) 27 yo female participant with good ITD digit segregation and an older (right) 68 yo female participant with poor ITD digit segregation.

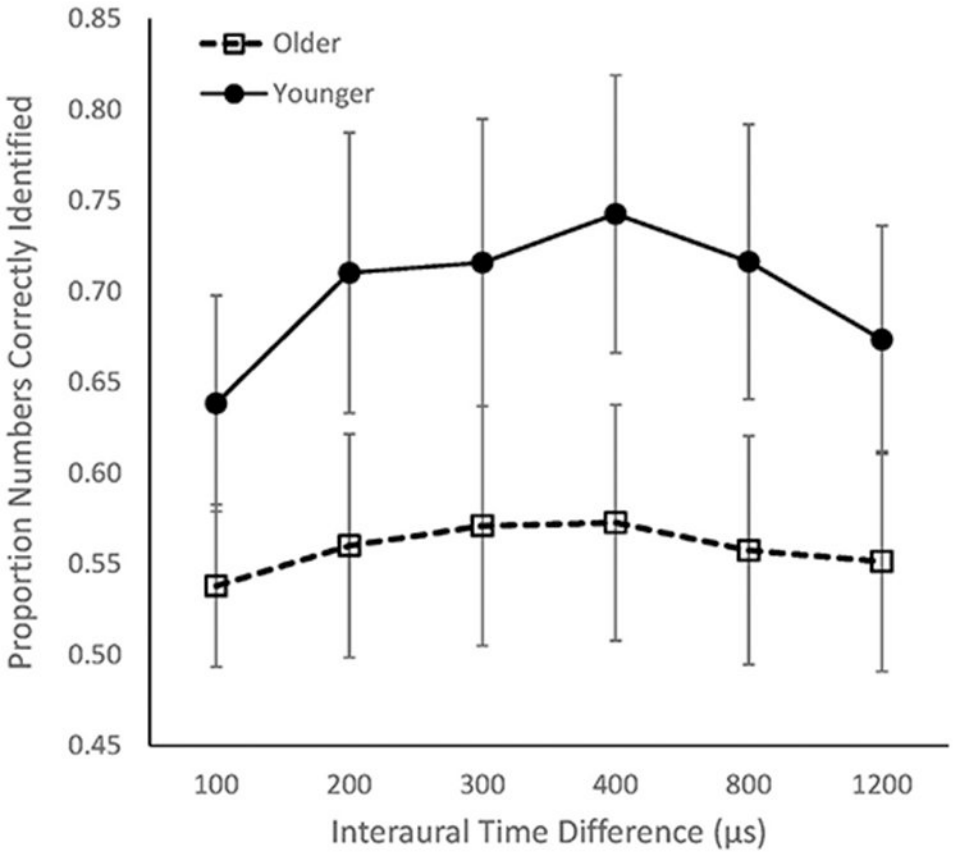

Fig. 5.

The proportion of numbers correctly sequentially identified in the ITD digit segregation task by older and younger listeners. Open squares indicate older listeners and filled circles indicate younger listeners. Error bars indicate 95% confidence intervals.

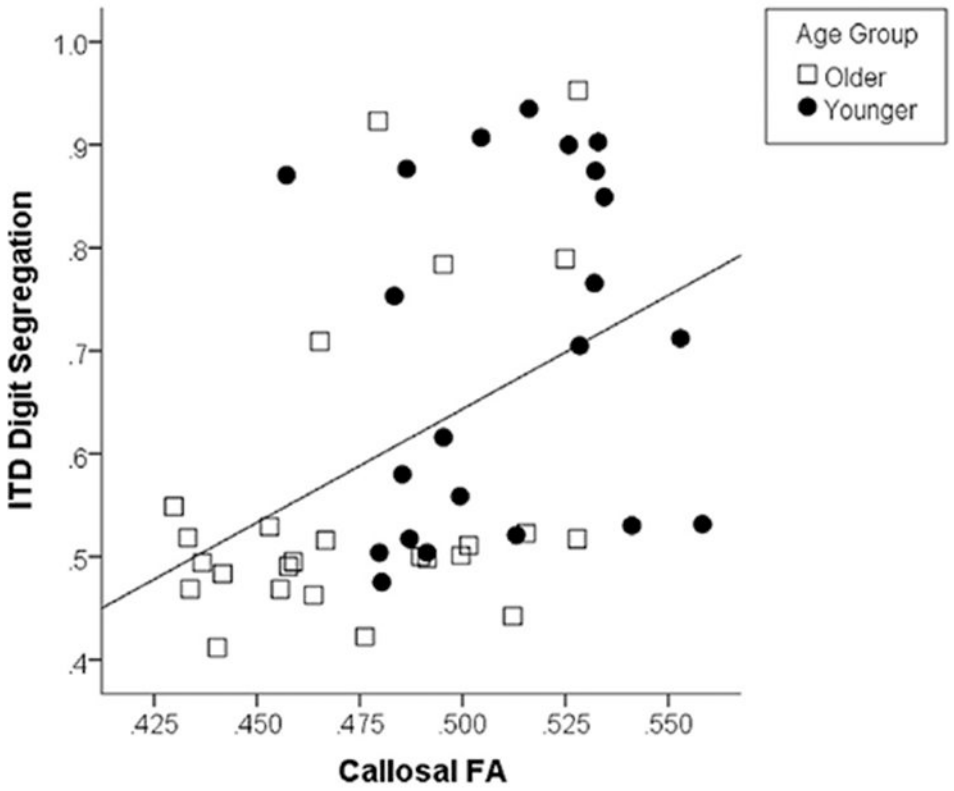

Fig. 6.

Scatter plot representing the relationship between callosal FA and ITD digit segregation. Open squares indicate older listeners and filled circles indicate younger listeners. The solid line represents a significant positive relationship across age-groups.

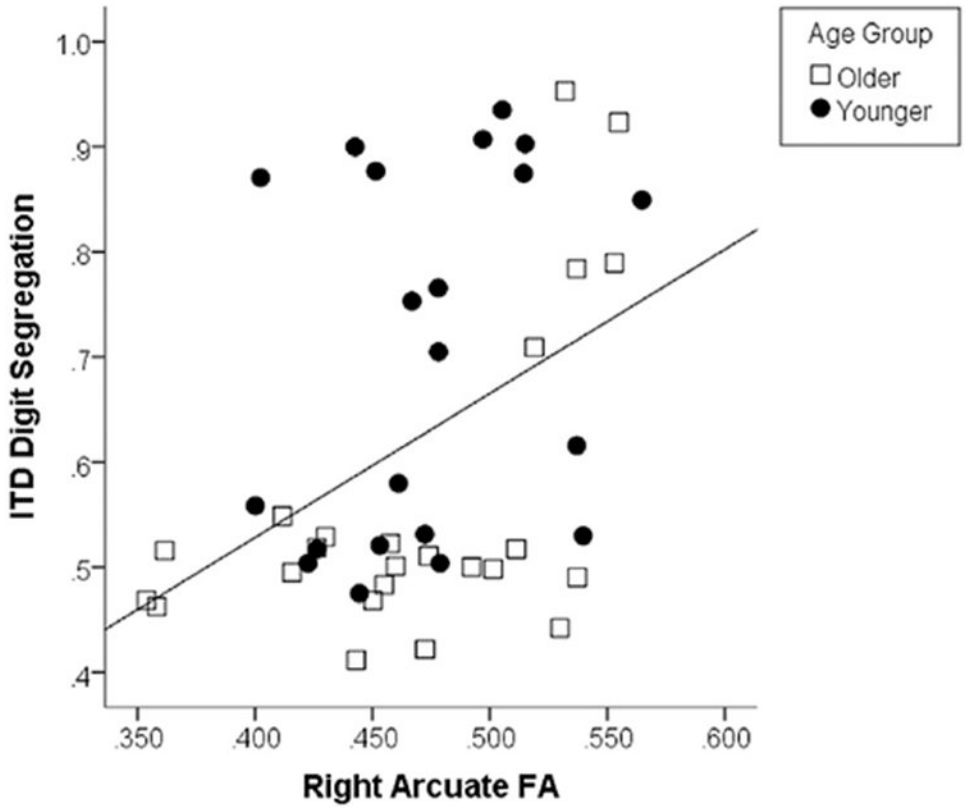

Fig. 7.

Scatter plot representing the relationship between right arcuate FA and ITD digit segregation. Open squares indicate older listeners and filled circles indicate younger listeners. The solid line represents a significant positive relationship across age-groups.

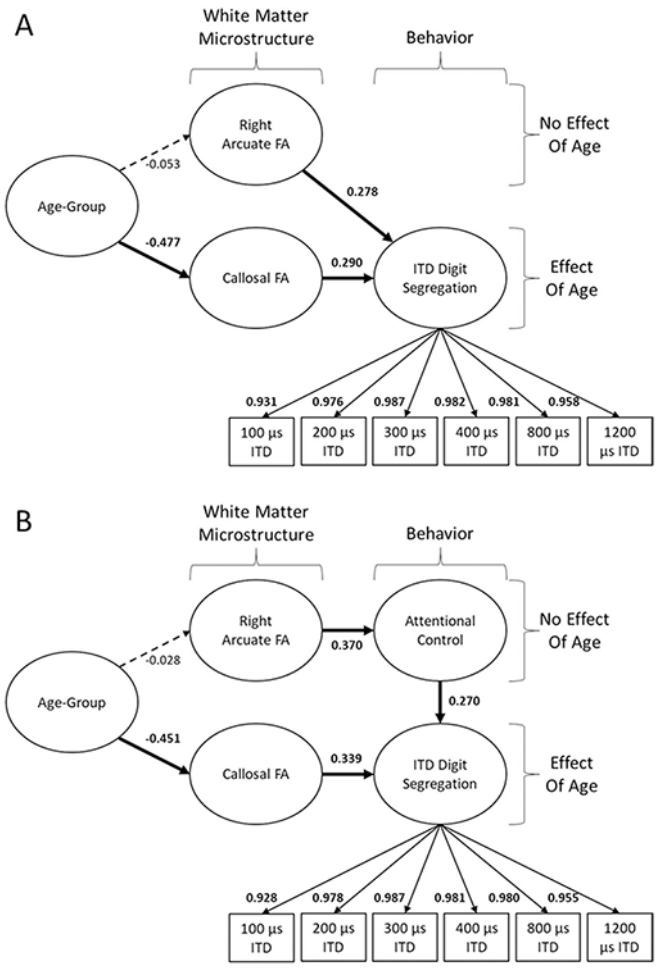

Fig. 8.

A) The structural equation model (SEM) used to test the degree to which callosal FA and arcuate FA mediate age-group differences in ITD digit segregation. B) The SEM in A modified to include attentional control as a potential mediator of the relationship between right arcuate FA and ITD digit segregation. Bold values represent significant model parameters.

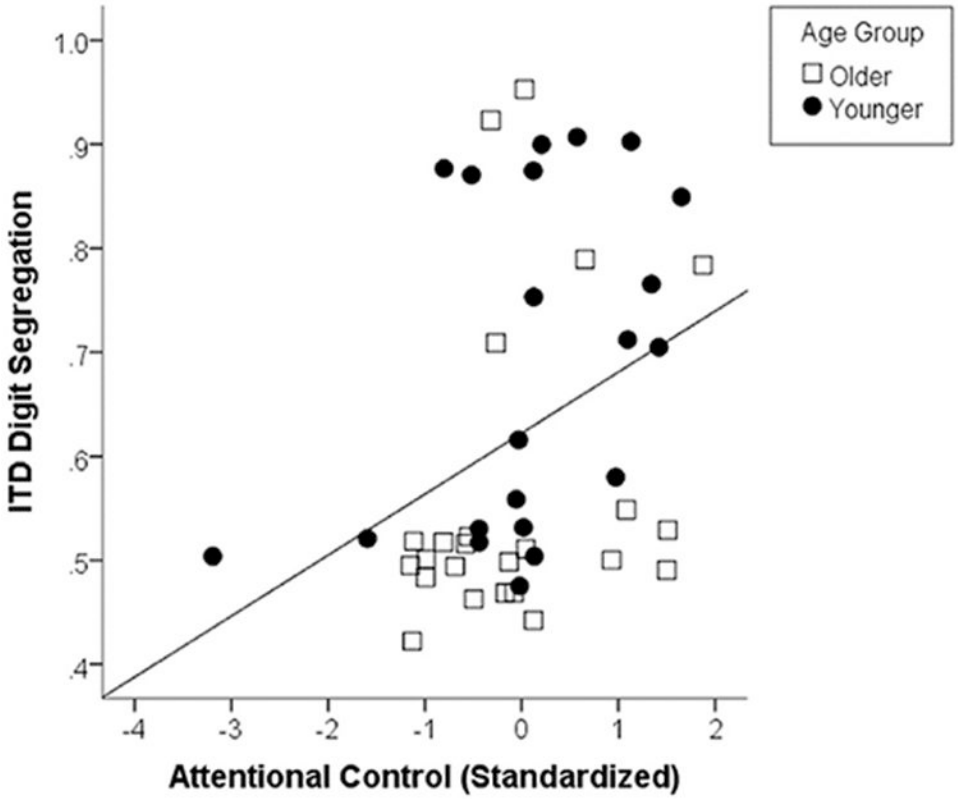

Fig. 9.

Scatter plot representing the relationship between attentional control (standardized residuals after regressing simple connections scores from complex connections scores) and ITD digit segregation. Open squares indicate older listeners and filled circles indicate younger listeners. The solid line represents a significant positive relationship across age-groups.

Table 1

Correlations between measures illustrating the covariance among outcome and predictor variables for LMER and SEM analyses.

Measure		n	M	SE	1		*1†*		2		3		4		5		6	7
1	ITD Digit Identification	47	0.624	0.025	–		–											
2	Age Group	47	0.530	0.074	−0.414	**			–									
3	Attentional Control	45	0.000	0.147	0.349	**			−0.077		–							
4	Perceptuomotor Processing Speed	45	29.056	1.203	0.231				−0.651	***	0.000		–					
5	Right-Ear Audiometric Threshold	47	7.016	1.050	−0.352	**			0.818	***	−0.141		−0.560	***	–			
6	Left-Ear Audiometric Threshold	47	8.372	1.131	−0.331	**			0.760	***	−0.147		−0.492	***	0.859	***	–	
7	SNR Loss (Quick SIN)	41	0.421	0.197	−0.243				0.039		−0.210		−0.254		0.101		0.101	–
8	Whole-Brain White Matter FA	47	0.355	0.006	0.379	**			−0.430	**	0.271	*	0.411	**	−0.163		−0.130	−0.167
9	Whole-Brain White Matter MD	47	0.622	0.007	−0.429	**			0.400	**	−0.246		−0.451	***	0.198		0.142	0.190
10	Corpus Callosum FA	47	0.491	0.005	0.440	***	0.335	*	−0.511	***	0.252		0.375	***	−0.311	*	−0.214	−0.193
11	Corpus Callosum MD	47	0.636	0.009	−0.351	**	−0.158		0.336	*	−0.109		−0.369	**	0.174		0.093	0.175
12	Right Arcuate FA	45	0.471	0.008	0.421	**	0.287	*	−0.053		0.370	**	0.106		0.017		0.136	−0.211
13	Right Arcuate MD	45	0.525	0.007	−0.339	*	−0.055		0.212		−0.168		−0.321	*	0.019		−0.043	0.151
14	Left Arcuate FA	47	0.495	0.008	0.233		0.004		−0.086		0.259	*	0.155		−0.030		0.134	−0.169
15	Left Arcuate MD	47	0.528	0.007	−0.381	**	−0.189		0.192		−0.155		−0.315	*	0.023		−0.065	0.135
16	Right SLF FA	47	0.484	0.010	0.343	**	0.155		−0.355	**	0.302	*	0.306	*	−0.182		−0.014	−0.125
17	Right SLF MD	47	0.519	0.007	−0.264	*	0.071		0.143		−0.097		−0.264	*	−0.105		−0.209	0.129
18	Left SLF FA	46	0.451	0.010	0.316	*	0.155		−0.396	**	0.227		0.345	*	−0.172		0.078	−0.089
19	Left SLF MD	46	0.524	0.007	−0.343	**	−0.107		0.093		−0.119		−0.194		−0.028		−0.182	0.116

Notes:

*
p < 0.05

**
p < 0.01

***
p < 0.001

ad hoc 1-tailed tests. Age group was number coded (younger = 0, older = 1). ITD Digit Segregation is averaged across ITDs. Processing speed = connections simple scores. Attentional Control = connections complex scores with connections simple scores regressed out. Correlations between different white matter metrics are not reported as all were moderately to strongly associated with one another (p < 0.004).

1†
correlations corrected for Whole Brain White Matter Microstructure (FA and MD).

Table 2

Parameter estimates for the structural equation model (SEM) testing the mediation effects of callosal FA and right arcuate FA on age-group differences in ITD digit segregation.

Parameter Estimate	B	SE	β	SE	z	p
Measurement Model Estimates						
Spatial Hearing → ITD 100 ms	1.000	0.000	0.931	0.020	45.844	<0.001
Spatial Hearing → ITD 200 ms	1.426	0.096	0.976	0.008	126.417	<0.001
Spatial Hearing → ITD 300 ms	1.479	0.094	0.987	0.005	204.556	<0.001
Spatial Hearing → ITD 400 ms	1.493	0.097	0.982	0.006	164.047	<0.001
Spatial Hearing → ITD 800 ms	1.442	0.094	0.981	0.006	155.790	<0.001
Spatial Hearing → ITD 1200 ms	1.228	0.090	0.958	0.013	74.703	<0.001
Error in ITD 100	0.002	0.001	0.132	0.038	3.499	<0.001
Error in ITD 200	0.001	0.000	0.047	0.015	3.116	0.002
Error in ITD 300	0.001	0.000	0.026	0.010	2.757	0.006
Error in ITD 400	0.001	0.000	0.035	0.012	2.958	0.003
Error in ITD 800	0.001	0.000	0.037	0.012	2.994	0.003
Error in ITD 1200	0.002	0.000	0.082	0.025	3.329	0.001
Error in ITD Digit Segregation	0.012	0.003	0.835	0.100	8.340	<0.001
Error in Callosal FA	0.001	0.000	0.773	0.103	7.473	<0.001
Error in Right Arcuate FA	0.003	0.001	0.997	0.016	62.882	<0.001
Error in Age-Group	0.249	0.000	1.000	0.000	NA	NA
Structural Model						
Age-Group → Callosal FA	−0.031	0.008	−0.477	0.108	−4.396	<0.001
Age-Group → Right Arcuate FA	−0.006	0.016	−0.053	0.149	−0.359	0.719
Callosal FA → ITD Digit Segregation	1.094	0.521	0.290	0.131	2.204	0.028
Right Arcuate FA → ITD Digit Segregation	0.645	0.319	0.278	0.132	2.110	0.035

Note: $\chi^2(26) = 64.114$, $p < 0.001$, AIC = −1084.587, BIC = −1052.067.

Table 3

Parameter estimates for the structural equation model (SEM) testing the mediation effects of callosal FA and attentional control on age-group differences in ITD digit segregation.

Parameter Estimate	B	SE	β	SE	z	p
Measurement Model Estimates						
Spatial Hearing → ITD 100 ms	1.000	0.000	0.928	0.022	42.394	<0.001
Spatial Hearing → ITD 200 ms	1.482	0.103	0.978	0.007	134.155	<0.001
Spatial Hearing → ITD 300 ms	1.520	0.101	0.987	0.005	201.581	<0.001
Spatial Hearing → ITD 400 ms	1.528	0.105	0.981	0.006	151.213	<0.001
Spatial Hearing → ITD 800 ms	1.469	0.102	0.980	0.007	142.155	<0.001
Spatial Hearing → ITD 1200 ms	1.248	0.097	0.955	0.014	67.547	<0.001
Error in ITD 100	0.002	0.001	0.140	0.041	3.443	0.001
Error in ITD 200	0.001	0.000	0.043	0.014	2.998	0.003
Error in ITD 300	0.001	0.000	0.026	0.010	2.667	0.008
Error in ITD 400	0.001	0.000	0.037	0.013	2.924	0.003
Error in ITD 800	0.001	0.000	0.040	0.014	2.964	0.003
Error in ITD 1200	0.002	0.000	0.089	0.027	3.282	0.001
Error in ITD Digit Segregation	0.011	0.003	0.811	0.106	7.675	<0.001
Error in Callosal FA	0.001	0.000	0.796	0.104	7.664	<0.001
Error in Right Arcuate FA	0.003	0.001	0.999	0.008	117.617	<0.001
Error in Attentional Control	0.829	0.179	0.863	0.097	8.858	<0.001
Error in Age-Group	0.249	0.000	1.000	0.000	NA	NA
Structural Model						
Age-Group → Callosal FA	−0.029	0.009	−0.451	0.115	−3.923	<0.001
Age-Group → Right Arcuate FA	−0.003	0.016	−0.028	0.152	−0.183	0.855
Right Arcuate FA → Attentional Control	6.771	2.591	0.370	0.132	2.813	0.005
Callosal FA → ITD Digit Segregation	1.258	0.517	0.339	0.130	2.604	0.009
Attentional Control → ITD Digit Segregation	0.033	0.017	0.270	0.134	2.026	0.043

Note: $\chi^2(34) = 62.947$, p = 0.002, AIC = −915.352, BIC = −880.128.

Table 4

Age-group correlations with the FA of different callosal tracts.

Measure		n	M	SE	1	
1	Age-Group	47	0.530	0.074	–	
2	Prefrontal Callosal Tract	47	0.563	0.009	−0.691	***
3	Superior Frontal Callosal Tract	46	0.552	0.009	−0.531	***
4	Motor Callosal Tract	45	0.577	0.010	−0.496	***
5	Somatosensory Callosal Tract	42	0.553	0.009	−0.584	***
6	Superior Parietal Callosal Tract	45	0.550	0.012	−0.419	**
7	Posterior Parietal Callosal Tract	46	0.545	0.011	−0.508	***
8	Occipital Callosal Tract	47	0.718	0.009	−0.369	**
9	Temporal Callosal Tract	46	0.592	0.007	−0.040	

Notes:

* $p < 0.05$

** $p < 0.01$

*** $p < 0.001$

ad hoc 1-tailed tests. Age group was number coded (younger = 0, older = 1).

Table 5

Parameter estimates for the structural equation model (SEM) testing the mediation effects of different callosal fiber tracts on age-group differences in ITD digit segregation.

SEM Parameter Estimates	B	SE	β	SE	z	p
Anterior Frontal						
Age-Group → Callosal FA	−0.077	0.012	−0.679	0.071	−9.615	<0.001
Age-Group → Right Arcuate FA −0.006	−0.006	0.016	−0.053	0.149	−0.359	0.719
Callosal FA → ITD Digit Segregation	0.619	0.293	0.281	0.127	2.215	0.027
Right Arcuate FA → ITD Digit Segregation	0.898	0.317	0.378	0.123	3.078	0.002
$\chi^2(26) = 40.519$, p = 0.035, AIC = −1051.288, BIC = −1018.768.						
Superior Frontal						
Age-Group → Callosal FA	−0.055	0.014	−0.501	0.106	−4.744	<0.001
Age-Group → Right Arcuate FA	−0.004	0.016	−0.036	0.151	−0.239	0.811
Callosal FA → ITD Digit Segregation	0.555	0.313	0.243	0.133	1.833	0.067
Right Arcuate FA → ITD Digit Segregation	0.844	0.327	0.356	0.128	2.775	0.006
$\chi^2(26) = 38.033$, p = 0.060, AIC = −1012.179, BIC = −980.064.						
Motor						
Age-Group → Callosal FA	−0.061	0.017	−0.473	0.112	−4.232	<0.001
Age-Group → Right Arcuate FA	−0.003	0.016	−0.027	0.152	−0.178	0.859
Callosal FA → ITD Digit Segregation	0.419	0.273	0.216	0.138	1.572	0.116
Right Arcuate FA → ITD Digit Segregation	0.767	0.330	0.329	0.133	2.473	0.013
$\chi^2(26) = 49.353$, p = 0.004, AIC = −972.209, BIC = −940.508.						
Somatosensory						
Age-Group → Callosal FA	−0.069	0.015	−0.574	0.097	−5.931	<0.001
Age-Group → Right Arcuate FA	−0.002	0.017	−0.022	0.158	−0.141	0.888
Callosal FA → ITD Digit Segregation	0.343	0.312	0.159	0.142	1.116	0.265
Right Arcuate FA → ITD Digit Segregation	0.939	0.348	0.393	0.132	2.963	0.003
$\chi^2(26) = 35.694$, p = 0.097, AIC = −905.436, BIC = −875.036.						
Superior Parietal						
Age-Group → Callosal FA	−0.065	0.022	−0.409	0.122	−3.362	0.001
Age-Group → Right Arcuate FA	−0.005	0.016	−0.049	0.152	−0.322	0.748
Callosal FA → ITD Digit Segregation	0.191	0.225	0.118	0.138	0.856	0.392
Right Arcuate FA → ITD Digit Segregation	0.975	0.338	0.405	0.127	3.186	0.001
$\chi^2(26) = 36.595$, p = 0.081, AIC = −951.040, BIC = −919.338.						
Posterior Parietal						
Age-Group → Callosal FA	−0.071	0.019	−0.484	0.108	−4.466	<0.001
Age-Group → Right Arcuate FA	−0.001	0.015	−0.008	0.151	−0.056	0.955
Callosal FA → ITD Digit Segregation	0.527	0.234	0.309	0.130	2.372	0.018
Right Arcuate FA → ITD Digit Segregation	0.759	0.338	0.308	0.130	2.367	0.018
$\chi^2(26) = 43.775$, p = 0.016, AIC = −996.299, BIC = −964.184.						
Occipital						

SEM Parameter Estimates	B	SE	β	SE	z	p
Age-Group → Callosal FA	−0.042	0.017	−0.345	0.127	−2.705	0.007
Age-Group → Right Arcuate FA	−0.006	0.016	−0.053	0.149	−0.359	0.719
Callosal FA → ITD Digit Segregation	0.392	0.283	0.191	0.136	1.409	0.159
Right Arcuate FA → ITD Digit Segregation	0.794	0.325	0.339	0.130	2.611	0.009
$\chi^2(26) = 53.928$, p = 0.001, AIC = −1021.153, BIC = −988.633.						
Temporal						
Age-Group → Callosal FA	0.001	0.015	0.008	0.151	0.052	0.959
Age-Group → Right Arcuate FA	−0.006	0.016	−0.055	0.150	−0.368	0.713
Callosal FA → ITD Digit Segregation	−0.229	0.362	−0.085	0.134	−0.635	0.526
Right Arcuate FA → ITD Digit Segregation	1.094	0.335	0.447	0.121	3.704	<0.001
$\chi^2(26) = 47.594$, p = 0.006, AIC = −1005.528, BIC = −973.413.						